Workpiece Vibration in Feed Direction Assisted Electrochemical Cutting Using Tube Electrode With Inclined Holes

Tao Yang
Nanjing university of aeronautics & astronautics
Xiaolong Fang
Nanjing university of aeronautics & astronautics
Yusen Hang
Nanjing university of aeronautics & astronautics
Zhengyang Xu
Nanjing university of aeronautics & astronautics
Yongbin Zeng (binyz@nuaa.edu.cn)
Nanjing university of aeronautics & astronautics

Research Article

Keywords: electrochemical cutting, tube electrode, inclined jet-flow holes, workpiece vibration

Posted Date: February 9th, 2021

DOI: https://doi.org/10.21203/rs.3.rs-162138/v1

Version of Record: A version of this preprint was published at The International Journal of Advanced Manufacturing Technology on July 12th, 2021. See the published version at https://doi.org/10.1007/s00170-021-07556-8.

Abstract

Electrochemical cutting using tube electrode with inclined holes is a machining method that directly and obliquely injects electrolyte into the machining gap through inclined jet-flow holes on the sidewall of a tube electrode, allowing the electrochemical cutting of a workpiece. To improve the machining efficiency and accuracy of this cutting technique, a method of workpiece vibration in feed direction assisted electrochemical cutting is proposed in which workpiece vibration along the feed direction rapidly and periodically changes the machining gap. The near-instantaneous increases in the machining gap promotes the waste electrolyte containing electrolytic products to flow down the machining gap. At the same time, the electrochemical reaction time under the non-uniform flow field caused by the inclined downward injection of electrolyte is reduced. The flow field simulation of electrolyte in machining gap indicates that the near-instantaneous increases in the machining gap can improve the flow velocity of electrolyte. Experiment demonstrates that the average feed rate can be increased by 50% and the machining efficiency is superior to that of electrochemical cutting assisted by workpiece non-vibration in feed direction. The difference between the upper and lower slit widths is reduced and the machining accuracy is improved. The effect of the vibrational amplitude and frequency on the machining result is also investigated. Finally, an array slice structure is fabricated on a stainless steel block with a cross-section of 10 mm × 10 mm at average feed rate of 6 mm/s using a vibrational amplitude and frequency of 0.1 mm and 1.5 Hz, respectively.

1 Introduction

With the emergence of various difficult-to-machine materials and their application in aerospace, precision instruments, die manufacturing, and other fields, more stringent requirements are being imposed on the efficiency and accuracy of mechanical processing. Consequently, appropriate processing and manufacturing techniques have become hot topics in current research [1]. Among precision machining techniques, electrochemical machining (ECM) has gained favor. ECM involves the local corrosion and removal of material from a metal workpiece in an electrolyte based on the principle of electrochemical anodic dissolution [2]. This enables a variety of metallic conductive materials to be processed without regard to the strength or hardness of the material itself, because the workpiece material is dissolved and removed in ionic form [3]. During processing, the cathode tool is always located away from the anode workpiece, and so no machining stress is generated. In addition, the tool cathode does not wear out, because it does not dissolve and only hydrogen bubbles are produced on its surface. The machined surface quality is good, and there is no recasting layer or thermal deformation because this is a cold machining method [4]. ECM has been applied in the manufacture of aero-engine blisks, casings, microprecision parts, and other key components [5, 6].

Wire electrochemical machining (WECM) is based on conventional ECM and uses a metal wire to cut the workpiece in a 2D plane [7]. This method not only inherits the advantages of conventional ECM, but also has its own unique benefits. A linear cathode with a simple structure is used, thus avoiding the complex

shaped cathode designs employed in conventional ECM, and thereby improving machining flexibility. WECM is suitable for the processing of high-precision 2.5-dimensional parts.

The limitation of mass transfer in narrow slits is a decisive factor that restricts the improvement of machining efficiency and accuracy [8, 9]. This is because the electrolytic products that remain in the machining gap change the electrolyte conductivity and negatively affect the distribution of the electric field in the machining gap, thus degrading the efficiency and accuracy of WECM. This problem becomes worse as the depth of the cutting slit increases, i.e., with increasing workpiece thickness. In recent years, a large number of studies have attempted to accelerate the removal of electrolytic products and refresh the electrolyte in the machining gap, thereby improving the machining efficiency and accuracy. For wire electrochemical micro-machining, the axial reciprocating vibration of a wire electrode has been proposed [10]. This uses the reciprocating vibration of the wire electrode to drag the electrolyte, promoting the removal of electrolytic products and the renewal of the electrolyte. A microscale square column tool array with a surface roughness of 0.058 μm was fabricated on an 80-μm-thick cobalt-based superalloy at a feed rate of 0.5 μm/s. Upward and downward reciprocating movement of the workpiece was found to induce a fluid flow in the electrolyte that aids the removal of electrolytic products. With this technique, a micro-gear structure was fabricated on an amorphous material, namely nickel-based metallic glass, at a feed rate of 0.5 μm/s [11]. The intermittent vibration of the electrode in the feed direction was observed to induce electrolyte flow in the machining gap, accelerating the removal of electrolytic products. This method has been proved to be effective in both simulations and experiments [12].

For the electrochemical cutting of thick workpieces, Volgin et al. [13] performed simulations that examined whether rotation or reciprocating movement of the cathode assisted electrochemical cutting and improved machining efficiency, especially if an electrode with a noncircular (e.g., square or triangular) cross-section was adopted. It has also been found [14] that using a ring of metal wire under unidirectional movement as the cathode drags the electrolyte, facilitating the rapid removal of electrolytic products and the refreshment of the electrolyte. Using this technique, groove and micro-star structures were fabricated on 5-mm-thick 304 stainless steel. Additionally, the use of a high-speed reciprocating traveling wire to accelerate the removal of electrolytic products from the machining gap enabled a curved slit structure to be fabricated on 20-mm-thick 304 stainless steel [15]. Zou et al. [16] processed a bar code on 5-mm-thick 304 stainless steel by WECM using vibrating ribbed wire tools, and achieved a feed rate of up to 1.5 μm/s. High-speed rotation of the electrode also induces the flow of electrolyte in the machining gap and promotes diffusion of the electrolytic products. A hollow structure of 3 mm thickness has been fabricated on 304 stainless steel using a high-speed rotary helical electrode at a feed rate of 6 μm/s [17]. In addition, a fir tree slot was fabricated using a cutting edge electrode at a feed rate of 6 μm/s on 5-mm-thick 304 stainless steel [18].

The auxiliary measures in the above research have improved the machining efficiency and machining ability of thick workpieces, but there is still room for improvement. Thus, ECM methods assisted by electrolyte flushing have been proposed. The high-velocity flow of electrolyte into the machining gap can flush electrolytic products rapidly from the gap and refresh the electrolyte [19]. Using two twisted metal

wires as cathodes, machining tests were carried out on 40-mm-thick direct-aged (DA) Inconel 718 with axial electrolyte flushing and a rotating cathode [20]. However, the top and bottom sides of the slit have quite different widths. In another approach, a linear metal tube with array holes replaces the conventional metal wire as the tool cathode, with electrolyte being injected directly into the machining gap through these holes to wash out electrolytic products [21]. A feed rate of 5 μm/s for a 10-mm-thick 304 stainless steel workpiece can be achieved with this technique. Yang et al. studied the effect of the holes spacing and inclination angle on the machining results. Through simulations and experiments, they found that the machining efficiency improved when the tube electrode with inclined holes was used for inner-jet electrochemical cutting. However, the problem of differences between the upper and lower slit widths persisted [22].

To improve the machining efficiency and reduce the difference between the upper and lower slit widths, a method of workpiece vibration in feed direction assisted electrochemical cutting using tube electrode with inclined jet-flow holes is proposed. Workpiece vibration along the feed direction rapidly and periodically changes the machining gap. The near-instantaneous increases in the machining gap promotes the waste electrolyte containing electrolytic products to flow down the machining gap. At the same time, the electrolytic reaction time under the non-uniform flow field caused by the inclined downward injection of electrolyte is reduced. The flow field simulation of electrolyte in machining gap indicates that the near-instantaneous increases in the machining gap can improve the flow velocity of electrolyte. Experiment demonstrates that the average feed rate can be increased by 50% and the machining efficiency is superior to that of electrochemical cutting assisted by workpiece non-vibration in feed direction. The difference between the upper and lower slit widths is reduced and the machining accuracy is improved. The effect of the vibrational amplitude and frequency on the machining result is also investigated. Finally, an array slice structure is fabricated on a stainless steel block with a cross-section of 10 mm × 10 mm at average feed rate of 6 μm/s using a vibrational amplitude and frequency of 0.1 mm and 1.5 Hz, respectively.

2 Machining Principle And Simulation Analysis

Figure 1 shows the machining principle of workpiece vibration in feed direction assisted electrochemical cutting using tube electrode with inclined holes. A linear metal tube with a closed bottom end and an array of inclined jet-flow holes on the tube wall acts as the tool cathode. The electrolyte passes through the inner cavity and the inclined jet-flow holes, and sprays directly onto the machining area to cause the electrochemical reaction and flush away electrolytic products. With the continuous feeding of the workpiece, a slit structure is produced on the workpiece.

In the electrochemical cutting process, workpiece vibration along the feed direction rapidly and periodically changes the machining gap. When the machining gap increases, the flow resistance of the electrolyte in the machining gap decreases, and the electrolyte injected downward at an inclined angle quickly flows out of the machining gap. When the machining gap reduces suddenly, the electrolyte ejected from the jet-flow holes is squeezed into the long and narrow machining gap instantly. A large

amount of electrolyte flows from the machining gap between the tube electrode and the workpiece to the machined slit, and then flows out of the slit along the back of the tube electrode. A small amount of electrolyte spills from the upper and lower ends of the machining gap. This constantly changes the spraying state of the electrolyte, which promotes the rapid removal of electrolytic products and the renewal of the electrolyte. At the same time, with the vibration of the workpiece, the spraying position of the high-flow-velocity electrolyte from the inclined jet-flow holes onto the machined surface changes continuously, which improves the uniformity of the flow field distribution in the machining gap (see Fig. 1(c)). In addition, the electrolytic reaction time under the non-uniform flow field caused by the inclined downward injection of electrolyte is reduced. This is beneficial to improving the machining accuracy.

Figure 2 shows the variations of the machining gap Δ_b with time t during workpiece vibratory. It is assumed that there is no contact between the workpiece and the tube electrode during the vibration. Backward vibration occurs when Δ_b increases from small to large values, and the end position of workpiece vibration is defined as the position at which Δ_b reaches its maximum value Δ_{b2}. Forward vibration occurs when Δ_b decreases from large to small values, and the starting position of workpiece vibration is defined as the position at which Δ_b reaches its minimum value Δ_{b1}. The vibrational amplitude of the workpiece is thus given by the distance between the starting position and the end position: $x' = \Delta_{b2} - \Delta_{b1}$.

To investigate the effect of workpiece vibration along the feed direction on electrolyte flow state in the machining gap, the flow field is simulated when the workpiece is in the end position under different vibrational amplitudes. A flow field model is established, as shown in Fig. 3. The vertical section A of the plane $Y = 0$ mm and the line L of 50 μm away from the workpiece machining surface are chosen to illustrate the different velocity distributions in electrochemical cutting. The calculation is performed by ANSY Fluent 17.0 based on the parameters listed in Table 1.

Table 1
Simulation parameters.

Diameter of tube cavity	**0.15 mm**
Thickness of tube wall	0.075 mm
Number of holes	10
Diameter of array holes	0.1 mm
Spacing of holes	1 mm
Machined length	0.75 mm
Slit width	0.5 mm
Vibrational amplitude	0, 0.1, 0.2, 0.3, 0.4 mm
Workpiece thickness	10 mm
Inlet pressure	2.0 MPa

Figure 4 shows the electrolyte flow velocity contours at different vibrational amplitudes. The results show that electrolyte always exists in the machining gap, which ensures normal electrochemical reaction, and that the electrolyte flows rapidly through the machining gap, facilitating rapid washing out of the electrolytic products.

Figure 5 is obtained by extracting and fitting the flow velocity on the line L at different vibrational amplitudes. On taking these results together with those in Fig. 4, it can be seen that the near-instantaneous increase in the machining gap leads to rapid flow of the electrolyte. This is because the electrolyte sprays onto the machining surface and bounces back into the machining gap. Finally, the electrolyte flows out from the upper and lower ends of the slit, and the side gap between the tube electrode and the workpiece. In the normal machining process, the flow resistance of electrolyte is great and the flow velocity is slow, since the machining gap between the tube electrode and the workpiece is very small. However, when the workpiece vibrates, and the machining gap becomes larger, the flow resistance decreases, and the electrolyte flows rapidly out of the machining gap along the lower end of the machined slit under the action of electrolyte internal pressure and gravity, as shown in Fig. 1(c).

3 Experimental Details

Figure 6 shows a schematic diagram of the workpiece vibration in feed direction assisted electrochemical cutting setup. To allow relative independence of the vibrational movement along the feed direction and the normal feed movement of the workpiece, as well as to ensure the machining efficiency of electrochemical cutting, this mode of coupling two kinds of movement is adopted. A high-precision motion stage (X'-axis) is added to the original three-axis (X/Y/Z-axis) machine tool. The workpiece is mounted on an anode clamp fixed to the motion stage of the machine tool, and the tube electrode is installed in a cathode clamp fixed to the pillar of the machine tool. The relative feed movement between

workpiece and cathode is driven by the X/Y-axis, the relative height between the workpiece and the jet-flow holes of the cathode is adjusted by the Z-axis, and the vibrational movement between workpiece and tube electrode is driven by the X'-axis.

The tool cathode is a commercial 304 stainless steel tube. Its closed end is machined by micro-laser welding and the array jet-flow holes are machined by micro-laser drilling. The outer and inner diameters of the tube cathode are 0.3 mm and 0.15 mm, respectively. There are 10 holes in the array, each with a diameter of 0.1 mm and which are spaced 1 mm apart. The array holes are inclined downward at an angle of 45°. The machining workpieces are ultrasonically cleaned 304 stainless steel pieces of size 60 mm (length) × 30 mm (width) × 10 mm (height). Table 2 summarizes the machining parameters applied in the experiment.

Table 2 Experimental parameters.

Electrolyte	$NaNO_3$
Concentration (g/L)	100
Inlet pressure (MPa)	2.0
Initial electrode gap (mm)	0.3
Vibrational amplitude (mm)	0, 0.1, 0.2, 0.3, 0.4
Vibrational frequency (Hz)	0.5, 1, 1.5, 2, 2.5
Electrical parameters	16 V, 35%, 50 kHz

For electrochemical cutting, the machining efficiency refers to the machined surface area of electrochemical cutting per unit time. The feed rate can be used to characterize the machining efficiency, because the thickness of the workpiece used in this study is constant. In the normal workpiece feed process, the variation in workpiece displacement is as shown in Fig. 7(a). In the process of workpiece vibration along the feed direction, the variation in workpiece displacement is as shown in Fig. 7(b). In the process of workpiece feeding and vibration, the variation in workpiece displacement is as shown in Fig. 7(c). In this study, the vibrational movement and feed movement of the workpiece is driven by the X'-axis and the X-axis, respectively. The movement of the X-axis determines the overall feed movement of the workpiece. The average feed rate of the workpiece is equal to the movement speed of the X-axis, although the actual feed rate of the workpiece varies periodically. During the experiment, the X-axis moves at the speed of 5 mm/s. To cut out 10 mm long slit for the processing task. If there is no short circuit in the whole process, increase the speed of X-axis (the increment is 0.5 mm/s) for the next cutting task. If there is a short circuit in the whole process, reduce the speed of X-axis (the decrement is 0.5 mm/s) for the next cutting task. Through many experiments, the maximum movement speed of X-axis under different machining conditions is obtained.

The machined slit structure is cleaned by ultrasonic and dried by wind. A digital microscope (DVM5000, Leica, Germany) and an optical microscope (SMT7-SFA, Olympus, Japan) are used to capture the shapes of the machined slit and measure the widths. The upper and lower surfaces of each slit are measured 10 times. The average slit width and the difference between the upper and lower slit widths are calculated. In this study, the slit width and the difference between the upper and lower slit widths are used to characterize the machining accuracy.

4 Results And Discussion

4.1 Effect of workpiece vibration in feed direction on electrochemical cutting

In order to verify the effect of the workpiece vibration in the feed direction on electrochemical cutting using tube electrode with inclined jet-flow holes, a comparative test of the workpiece non-vibration assisted electrochemical cutting and workpiece vibration (amplitude is 0.1 mm and frequency is 1.5 Hz) assisted electrochemical cutting was conducted. The results are presented in Fig. 8, and the cut slits at maximum movement speed of X-axis is shown in Fig. 9.

In the process of electrochemical cutting assisted by workpiece non-vibration in feed direction, the maximum movement speed of X-axis is 4 μm/s, and the machining efficiency is lower. This is because the machining gap between the tube electrode and the workpiece is very small during electrochemical cutting. The flow resistance of the electrolyte, which contains a large number of electrolytic products, is relatively large and the flow velocity is relatively slow, especially in the machining area that is not directly sprayed by the high-flow-velocity electrolyte ejected from the jet-flow holes. As a result, the conductivity of the electrolyte in the machining gap is low and the machining efficiency is poor.

In the process of electrochemical cutting assisted by workpiece vibration in feed direction, the maximum movement speed of X-axis is 6 μm/s, and the machining efficiency is higher, which is increased by 50% compared with that of electrochemical cutting assisted by workpiece non-vibration in feed direction. This is because the vibration of the workpiece in the feeding process changes rapidly and periodically the machining gap between the workpiece and tube electrode. When the machining gap increases, the flow resistance of the electrolyte decreases and the flow velocity becomes faster. The waste electrolyte is quickly flushed out of the machining gap. When the machining gap decreases, the electrolytic reaction between the workpiece and tube electrode occurs rapidly in the fresh electrolyte, and the workpiece material is quickly corroded and removed. Figure 10 shows the flow state of the electrolyte during workpiece vibration. When the machining gap increases, more electrolyte flows downward along the front side of the tube electrode, as shown in Fig. 10(a). When the machining gap decreases, more electrolyte flows out of the gap between the tube electrode and the slit sidewall, and then flows downward along the backside of the tube electrode, as shown in Fig. 10(b). In addition, the vibration of the workpiece periodically changes the spraying position of the high-flow-velocity electrolyte ejected from the jet-flow

holes on the machining surface, which allows the electrolytic products of the machining surface to be quickly removed.

As can be seen from Fig. 8(b), the slit cut by workpiece non-vibration electrochemical cutting is wider, while the slit cut by workpiece vibration assisted electrochemical cutting is narrower. This is because, in the process of electrochemical cutting, a lower feed rate implies a longer machining time per unit length, allowing more material to be removed from the sidewall of the slit and producing a wider slit. On the contrary, a faster feeding rate results in a shorter machining time per unit length, and so less material is removed from the sidewall of the slit and a narrower slit is produced.

By comparing the difference between the upper and lower widths of the cut slits (see Fig. 8(c)), it can be seen that electrochemical cutting assisted by workpiece non-vibration in feed direction gives a wide variation of 115.56 μm. This is because the electrolyte is ejected downward from the jet-flow holes at an inclined angle, and so the upper part of the machining gap has a low flow rate while the lower part has a high flow rate. This flow field distribution results in less material being removed at the upper end of the slit and more material being removed at the lower end. Thus, the cut slit is narrow at the upper end and wide at the lower end. In the process of electrochemical cutting assisted by workpiece vibration in feed direction, the vibration of the workpiece not only speeds up the renewal of the electrolyte due to the change in the machining gap, but also makes the flow field in the machining gap more uniform because of the change in the spraying height from the jet-flow holes to the machining surface. In addition, the continuous vibration of the workpiece shortens the electrochemical reaction time and reduces the influence of the uneven distribution of the electrolyte flow field on the consistency of slit width. As a result, the slit cut by electrochemical cutting assisted by workpiece vibration in feed direction has the smallest difference between the upper and lower widths, just 49.6 μm.

4.2 Effect of vibrational amplitude

To examine the effect of workpiece vibrational amplitude on electrochemical cutting, the vibrational frequency is fixed at 1 Hz. Figure 11 shows the variations in the maximum movement speed of X-axis and the slit width with respect to vibrational amplitude.

When the vibrational amplitude is greater than 0.1 mm, the maximum movement speed of X-axis gradually decreases as the amplitude increases. This is because, in the process of workpiece vibration, the vibrational frequency remains unchanged, that is, the time taken for the workpiece to move a stroke is the same. As the vibrational amplitude increases, the travel distance of the workpiece increases, and the reaction time between the workpiece and the tube electrode decreases under the conditions of a high current density and small machining gap. Therefore, less material is removed and the maximum movement speed of X-axis decreases. In addition, as the distance between the workpiece and the tube electrode increases, the position of the high-flow-velocity electrolyte ejected from the jet-flow holes to the machining surface becomes lower. A lower flow rate and lower flow velocity of electrolyte at the upper end of the machining gap result in a lower material removal rate at the upper end of the cutting slit. This limits the overall movement speed and reduces the machining efficiency. When the vibrational amplitude

is too large (0.4 mm), the flow rate of electrolyte at the upper end of the machining gap is too low to ensure the electrochemical reaction between the tube electrode and the workpiece, and the machining fails.

As can be seen from Fig. 11(b), when the vibrational amplitude is more than 0.1 mm, the slit width increases with increasing vibrational amplitude. This is determined by the feed rate. As can also be seen from Fig. 11(b), with an increase in vibrational amplitude, the difference between the upper and lower slit widths gradually increases. As the machining gap increases, a larger vibrational amplitude of the workpiece causes the machining surface to be farther from the tube electrode and lowers the spraying position of the high-flow-velocity electrolyte ejected from the jet-flow holes to the machining surface. A lower flow rate and lower flow velocity of the electrolyte in the upper part of the machining gap are associated with a greater flow rate and faster flow velocity of the electrolyte in the lower part. In the process of narrowing the machining gap, the electrolyte that is instantaneously squeezed into the machining gap has lower velocity on the top and higher velocity on the bottom. This distribution of the flow field causes the difference between the upper and lower slit widths to increase.

4.3 Effect of vibrational frequency

To examine the effect of workpiece vibrational frequency on electrochemical cutting, the vibrational amplitude is fixed at 0.1 mm. The variations in the maximum movement speed of X-axis and the slit width with respect to vibrational frequency are shown in Fig. 12.

It can be seen from Fig. 12 that the vibrational frequency has little effect on the machining results. When the vibrational amplitude is constant, changes in the vibrational frequency only affect the vibrational number of the workpiece, and have little effect on the overall flow field and electric field. However, when the vibrational frequency increases from 1 Hz to 1.5 Hz, the maximum movement speed of X-axis increases from 5.5 μm/s to 6 μm/s. This is because, as the vibrational frequency increases, the spraying number of the electrolyte hitting a given position on the machining surface increases, promoting the removal of electrolytic products and refreshing the electrolyte. The rapid removal of electrolytic products increases the conductivity of electrolyte in the machining gap, and so the current density increases and the material is removed at a faster rate. Similarly, for a given feed rate, an increase in frequency causes the slit width and the difference between the upper and lower slit widths to increase.

4.4 Fabrication of array slice structure

Using the optimized machining parameters, namely, a workplace vibration amplitude and frequency of 0.1 mm and 1.5 Hz, an array slice structure was fabricated on a 304 stainless steel block with a cross-section of 10 mm × 10 mm at average feed rate of 6 μm/s. The result is shown in Fig. 13. The average thickness of the array slice is 915.8 μm and the standard deviation of thickness is 29.5 μm.

5 Conclusions

To improve the machining efficiency and accuracy of electrochemical cutting using tube electrode with inclined jet-flow holes, this paper has described a method of workpiece vibration in feed direction assisted machining. A series of simulations and experimental tests lead to the following conclusions regarding the proposed method:

(1) During the process of electrochemical cutting assisted by workpiece vibration along the feed direction, the vibration rapidly and periodically changes the gap between the tube electrode and the workpiece, the spraying state of electrolyte on the machining surface, and the spraying position along the workpiece thickness. This can improve the flow velocity of electrolyte and promotes the waste electrolyte containing electrolytic products to flow down the machining gap.

(2) In the process of electrochemical cutting assisted by workpiece vibration along the feed direction, the average feed rate can be increased by 50% and the machining efficiency is superior to that of electrochemical cutting assisted by workpiece non-vibration in feed direction. The difference between the upper and lower slit widths is reduced and the machining accuracy is improved.

(3) The vibrational amplitude determines the changes in the machining gap and has a great influence on the machining result. The vibrational frequency determines the number of changes in the machining gap, but has only a weak influence on the machining result.

(4) Using the optimized machining parameters, an array slice structure has been fabricated on a 304 stainless steel block with a cross-section of 10 mm × 10 mm at average feed rate of 6 μm/s.

-

Declarations

Funding

This work was supported by the National Natural Science Foundation of China (91960204), the Natural Science Foundation of Jiangsu Province (BK20191279), the National Natural Science Foundation of China for Creative Research Groups (51921003), and the Postgraduate Research & Practice Innovation Program of Jiangsu Province (KYCX19_0167).

Competing Interests

The authors declare that they have no conflict of interest.

Ethical Approval

The article follows the guidelines of the Committee on Publication Ethics (COPE) and involves no studies on human or animal subjects.

Consent to Participate

Not applicable.

Consent to Publish

Not applicable.

Availability of data and materials

All data generated or analyzed during this study are included in this article.

Authors Contributions

Tao Yang conceived of the study, designed the study and collected the data. All authors analyzed the data and were involved in writing the manuscript.

References

1. Lauwers B, Klocke F, Klink A, et al (2014) Hybrid processes in manufacturing. CIRP Ann - Manuf Technol 63:561–583.
2. Rajurkar KP, Zhu D, McGeough JA, et al (1999) New Developments in Electro-Chemical Machining. CIRP Ann - Manuf Technol 48:567–579.
3. Lohrengel MM, Rataj KP, Münninghoff T (2016) Electrochemical Machining—mechanisms of anodic dissolution. Electrochim Acta 201:348–353.
4. Murali Sundaram, Rajurkar K, Zhang WW (2010) Electrical and Electrochemical Processes. Intell Energy F Manuf 173–212.
5. Klocke F, Klink A, Veselovac D, et al (2014) Turbomachinery component manufacture by application of electrochemical , electro-physical and photonic processes. CIRP Ann - Manuf Technol 63:703–726.
6. Lei GP, Zhu D, Zhu D (2021) Feeding strategy optimization for a blisk with twisted blades in electrochemical trepanning. J Manuf Process 62:591–599.
7. Shin HS, Kim BH, Chu CN (2008) Analysis of the side gap resulting from micro electrochemical machining with a tungsten wire and ultrashort voltage pulses. J Micromechanics Microengineering 18:1–6.

8. Saxena KK, Qian J, Reynaerts D (2018) A review on process capabilities of electrochemical micromachining and its hybrid variants. Int J Mach Tools Manuf 127:28–56.
9. Debnath S, B.Doloi Z, Bhattacharyya B (2019) Review—Wire Electrochemical Machining Process: Overview and Recent Advances. J Electrochem Soc 166:E293–E309.
10. Xu K, Zeng YB, Li P, et al (2016) Effect of wire cathode surface hydrophilia when using a travelling wire in wire electrochemical micro machining. J Mater Process Technol 235:68–74.
11. Zeng YB, Meng LC, Fang XL (2017) Surface characteristics of Ni-based metallic glass in wire electrochemical micro machining. J Electrochem Soc 164:E408–E421.
12. He HD, Zhang X, Qu NS, Zeng YB (2019) Wire Electrochemical Micro Machining Assisted with Coupling Axial and Intermittent Feed-Direction Vibrations. J Electrochem Soc 166:E165–E180.
13. Volgin VM, Lyubimov V V., Kukhar VD, Davydov AD (2015) Modeling of wire electrochemical micromachining. Procedia CIRP 37:176–181.
14. Zeng YB, Yu Q, Fang XL, et al (2015) Wire electrochemical machining with monodirectional traveling wire. Int J Adv Manuf Technol 78:1251–1257.
15. Qu NS, Ji HJ, Zeng YB (2014) Wire electrochemical machining using reciprocated traveling wire. Int J Adv Manuf Technol 72:677–683.
16. Zou XH, Fang XL, Chen M, Zhu D (2018) Investigation on mass transfer and dissolution localization of wire electrochemical machining using vibratory ribbed wire tools. Precis Eng 51:597–603.
17. Fang XL, Zhang PF, Zeng YB, et al (2016) Enhancement of performance of wire electrochemical micromachining using a rotary helical electrode. J Mater Process Technol 227:129–137.
18. Zou XH, Fang XL, Zeng YB, Zhu D (2017) A high efficiency approach for wire electrochemical micromachining using cutting edge tools. Int J Adv Manuf Technol 91:3943–3952.
19. Tyagi A, Sharma V, Jain V., Ramkumar J (2018) Investigations into side gap in wire electrochemical micromachining (wire-ECMM). Int J Adv Manuf Technol 94:4469–4478.
20. Klocke F, Herrig T, Zeis M, Klink A (2018) Experimental Investigations of Cutting Rates and Surface Integrity in Wire Electrochemical Machining with Rotating Electrode. Procedia CIRP 68:725–730.
21. Yang T, Zeng YB, Hang YS (2019) Workpiece reciprocating movement aided wire electrochemical machining using a tube electrode with an array of holes. J Mater Process Technol 271:634–644.
22. Yang T, Zeng YB, Sang YM, Li SY (2020) Effect of structural parameters of array of holes in the tube electrode for electrochemical cutting. Int J Adv Manuf Technol 107:205–216.

Figures

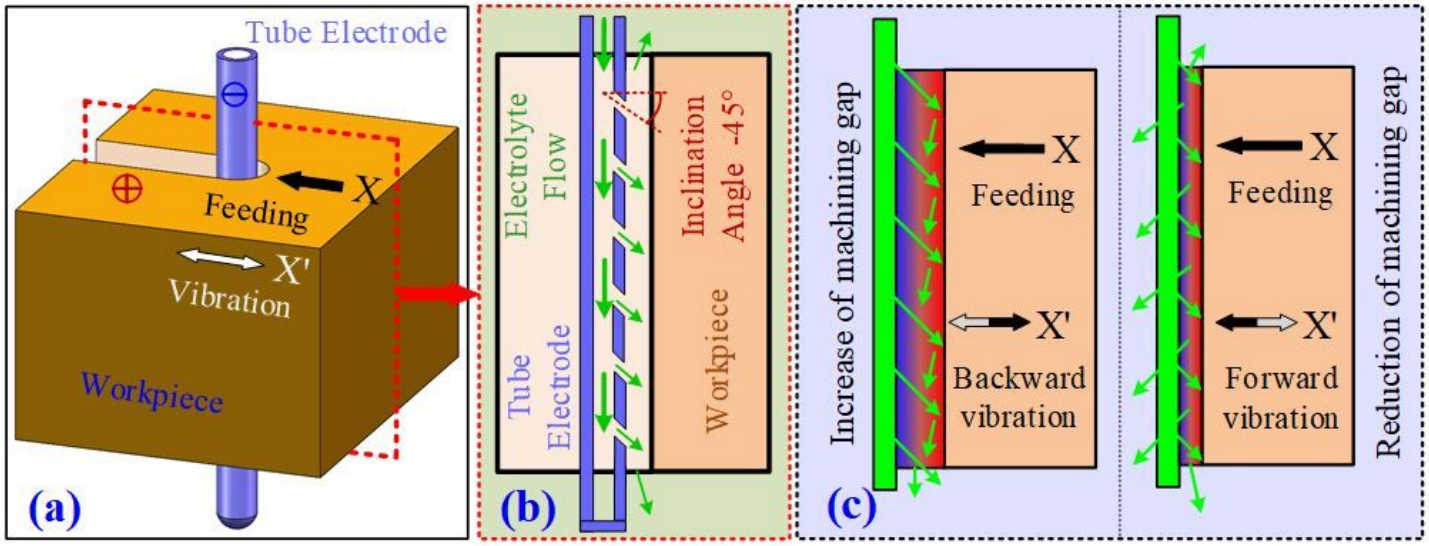

Figure 1

Workpiece vibration in feed direction assisted electrochemical cutting using tube electrode with inclined holes: (a) machining principle, (b) section view, (c) machining diagram showing backward and forward vibration of workpiece.

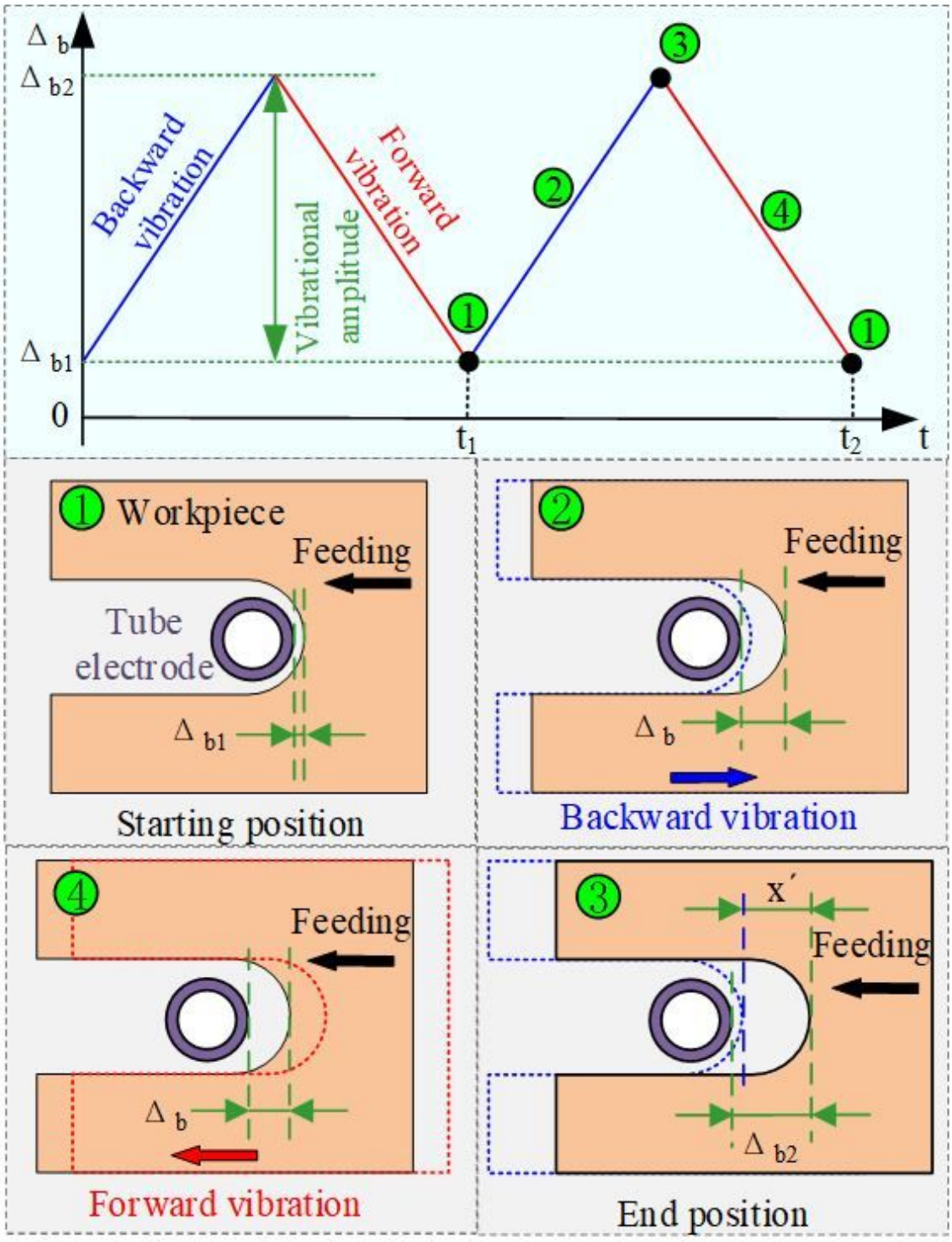

Figure 2

Variation of machining gap during workpiece vibration in the feed direction.

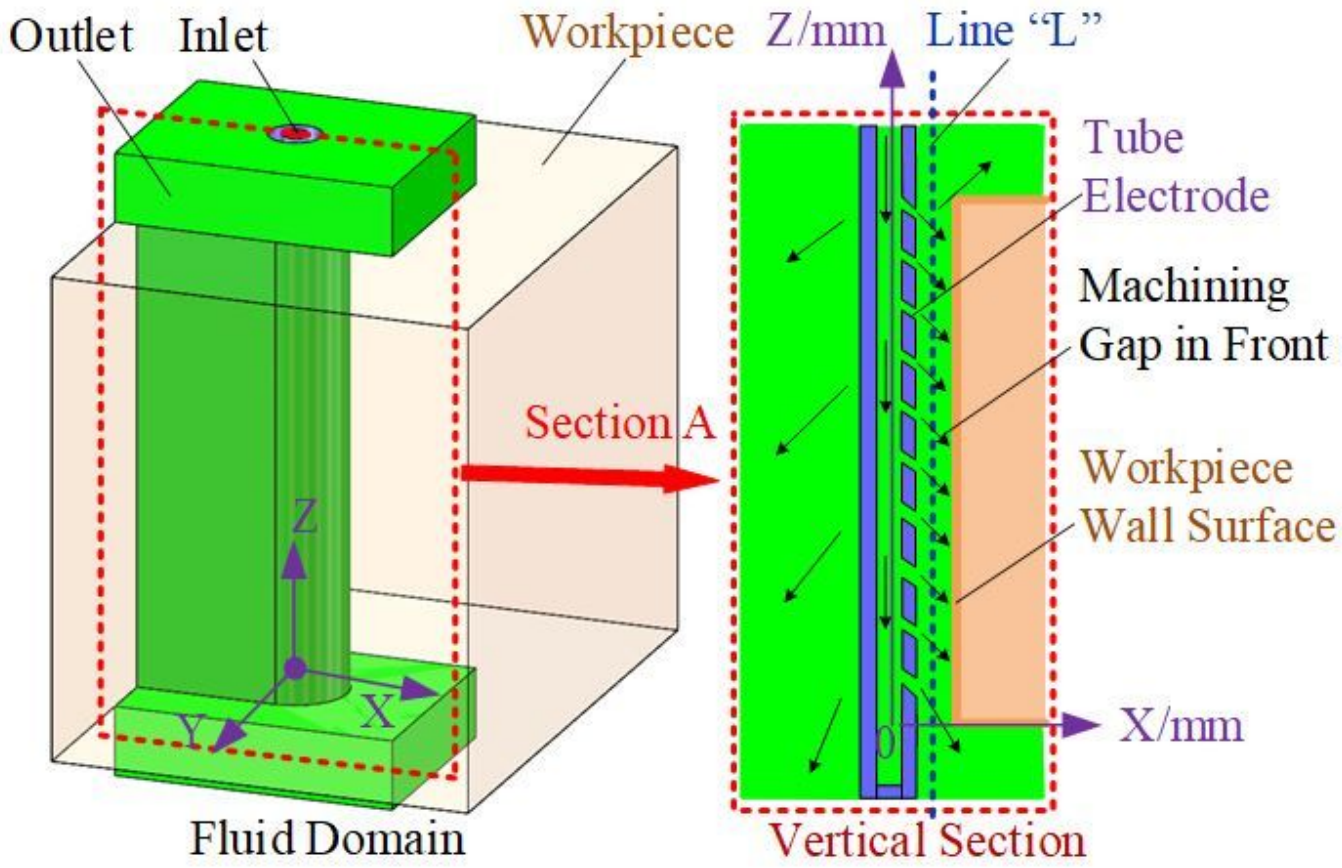

Figure 3

Simulation model of flow field in machining gap.

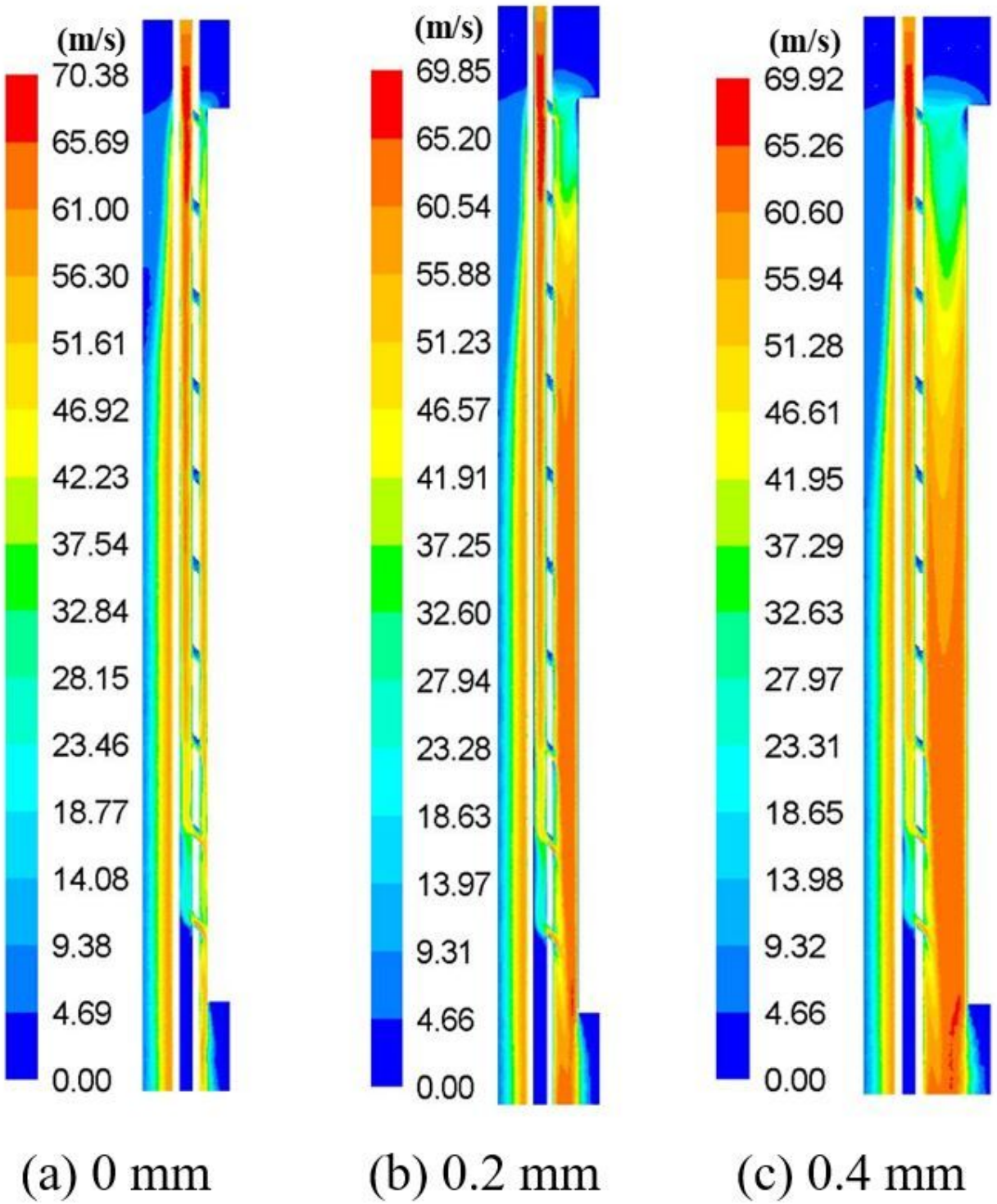

Figure 4

Electrolyte flow velocity contours for the different vibrational amplitudes: (a) 0 mm; (b) 0.2 mm; (c) 0.4 mm.

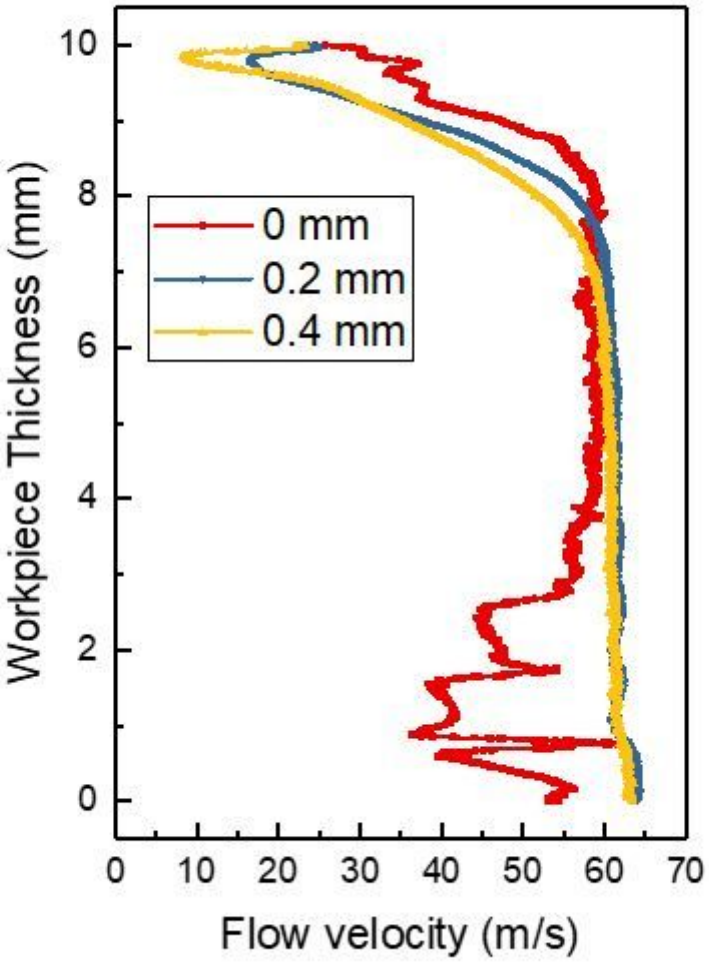

Figure 5

Electrolyte flow velocity on the line L at different vibrational amplitudes.

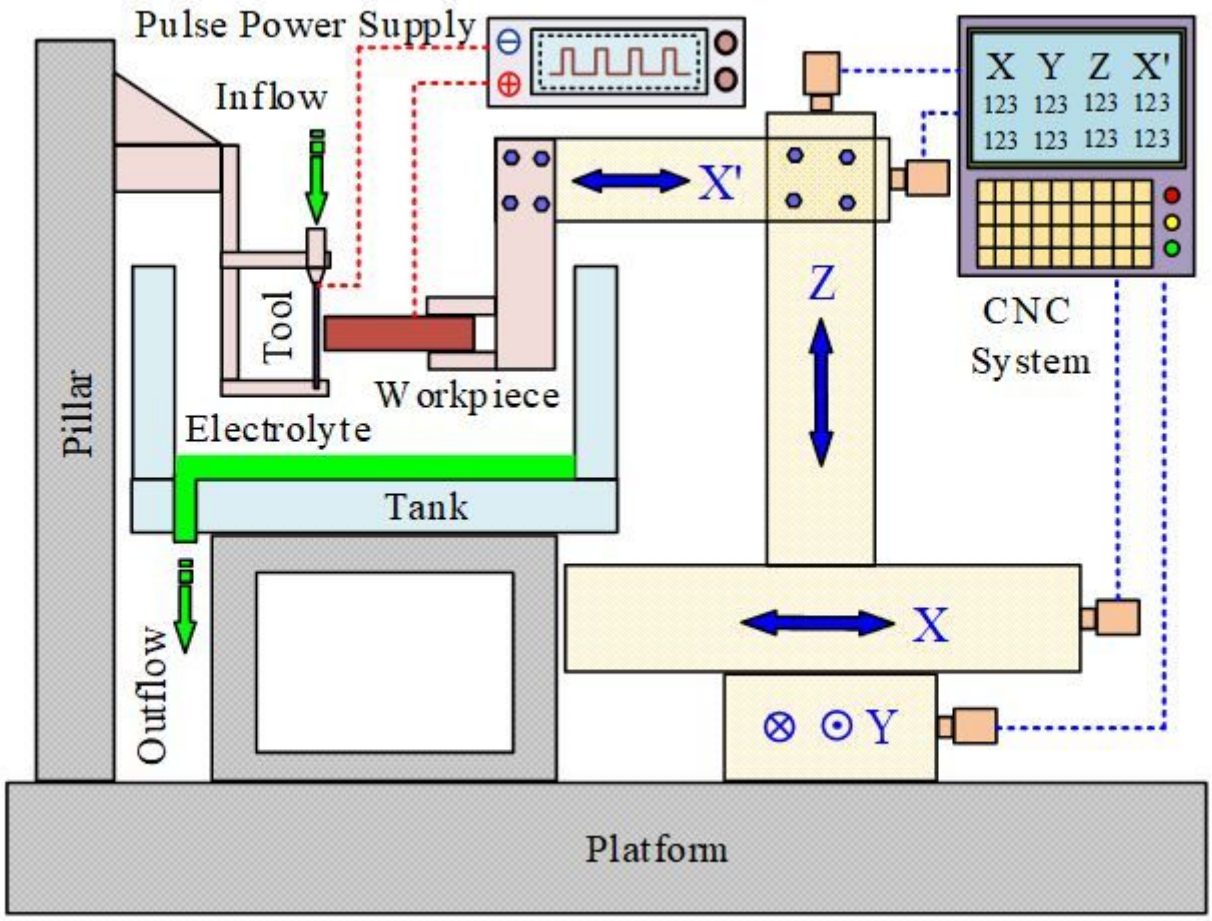

Figure 6

Schematic diagram of the experimental setup.

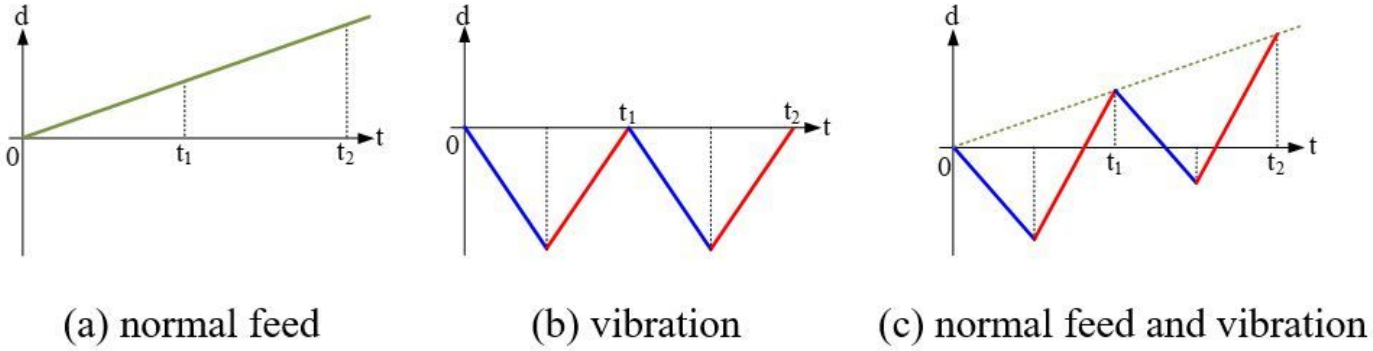

Figure 7

Variation of workpiece displacement during workpiece (a) normal feed, (b) vibration, and (c) normal feed and vibration.

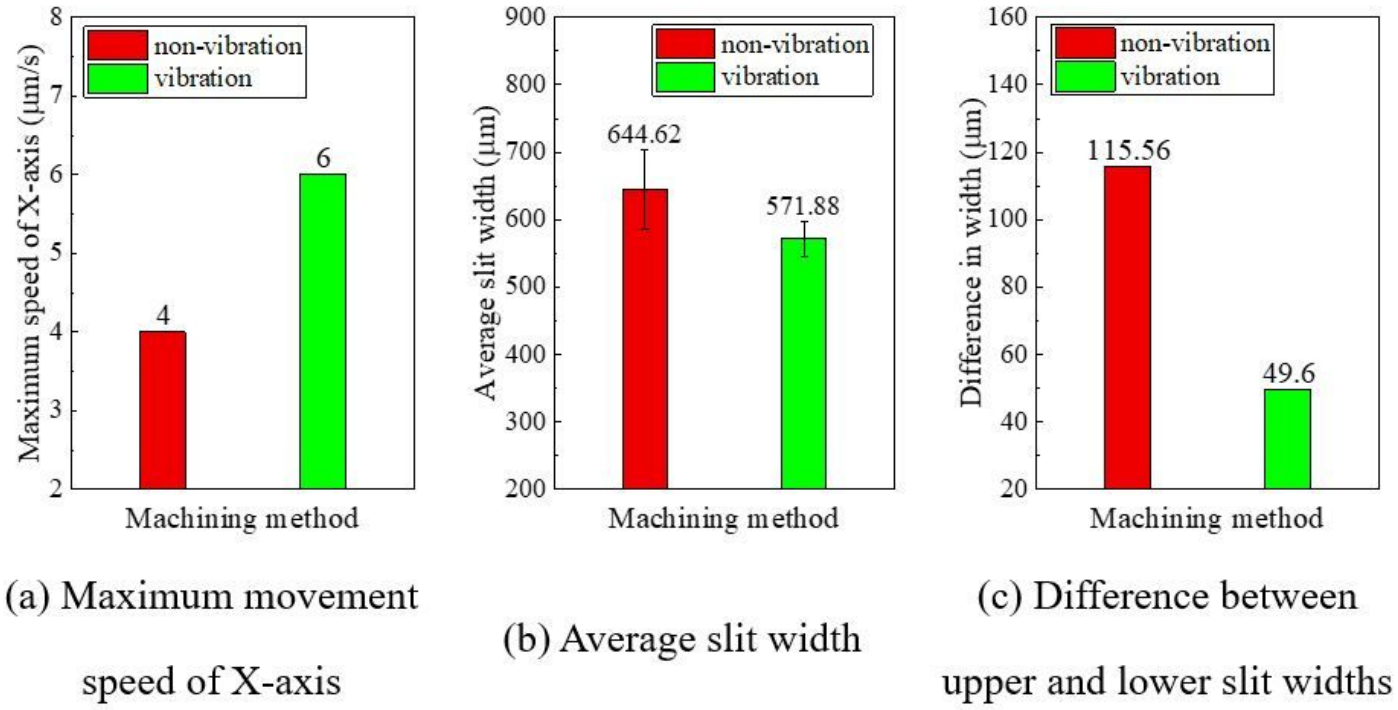

(a) Maximum movement speed of X-axis

(b) Average slit width

(c) Difference between upper and lower slit widths

Figure 8

Results of the different machining methods.

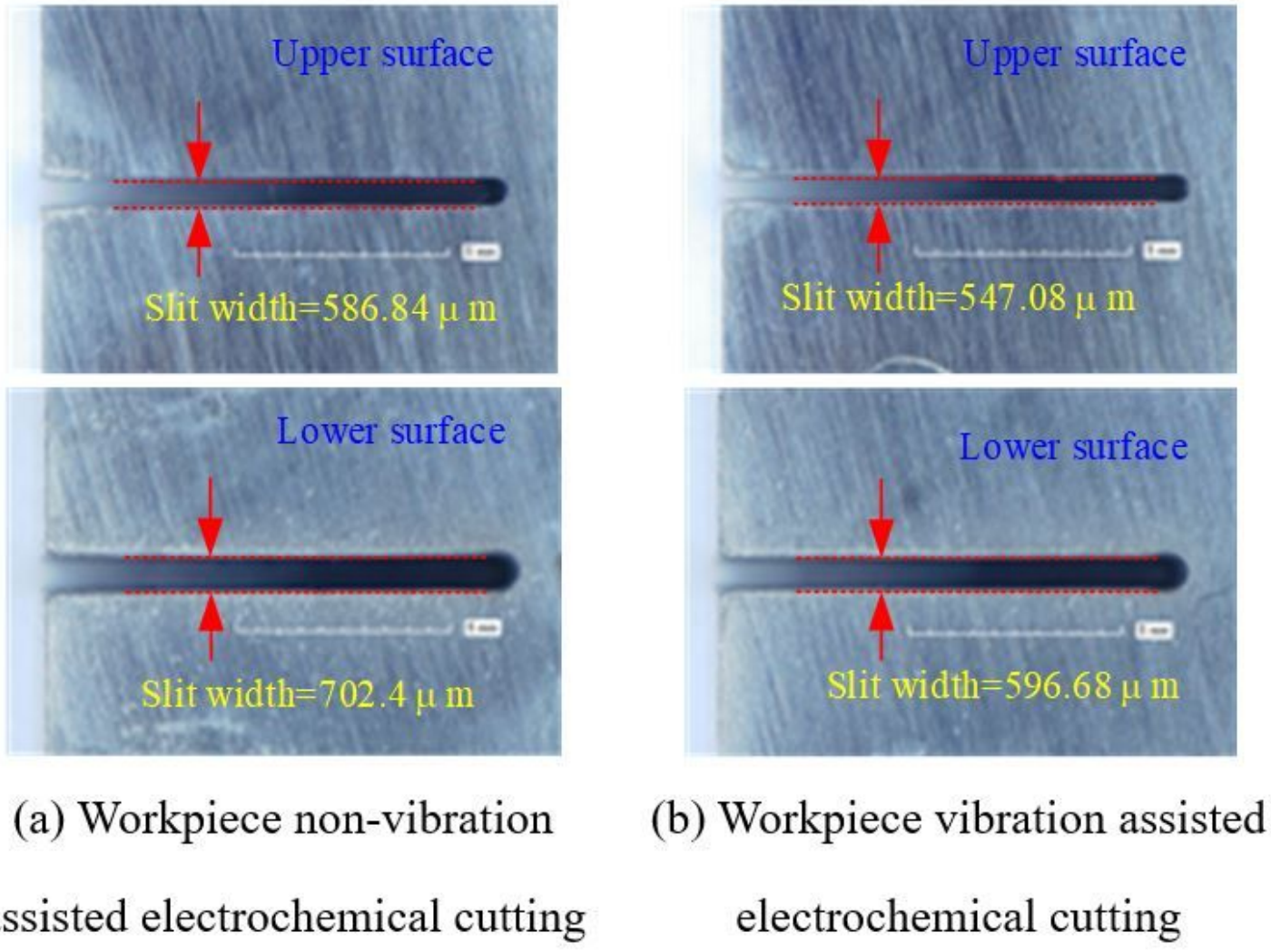

Figure 9

Slits cut by different machining methods.

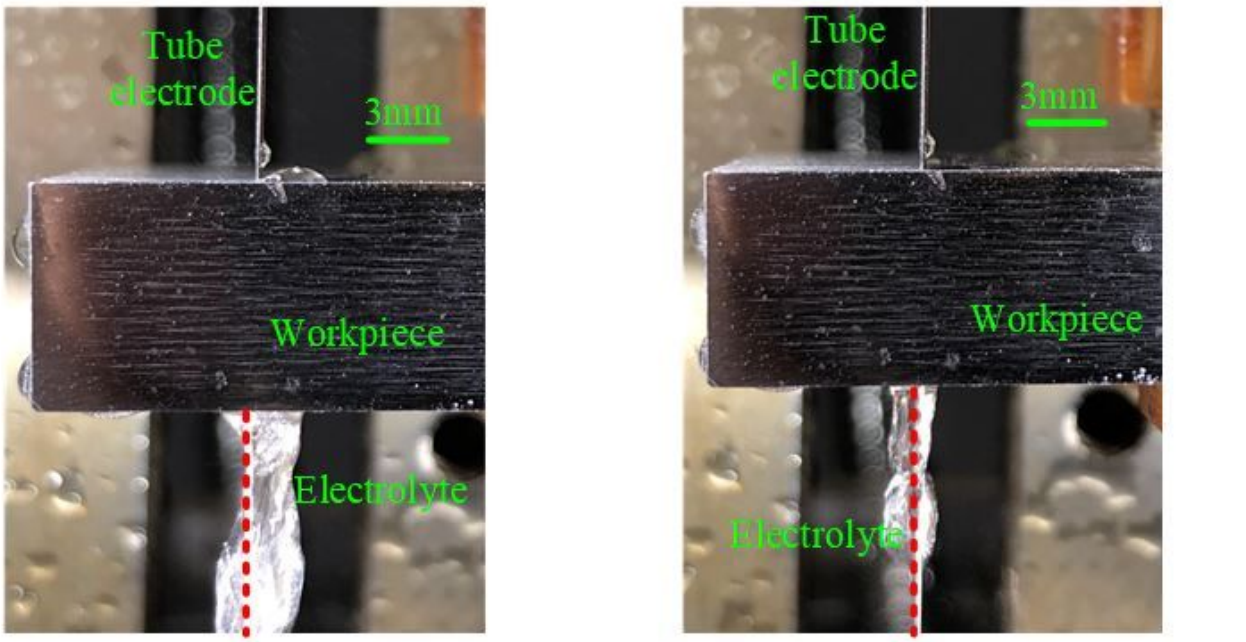

(a) When machining gap increases (b) When machining gap decreases

Figure 10

Electrolyte flow state during workpiece vibration: (a) When machining gap increases and (b) when machining gap decreases.

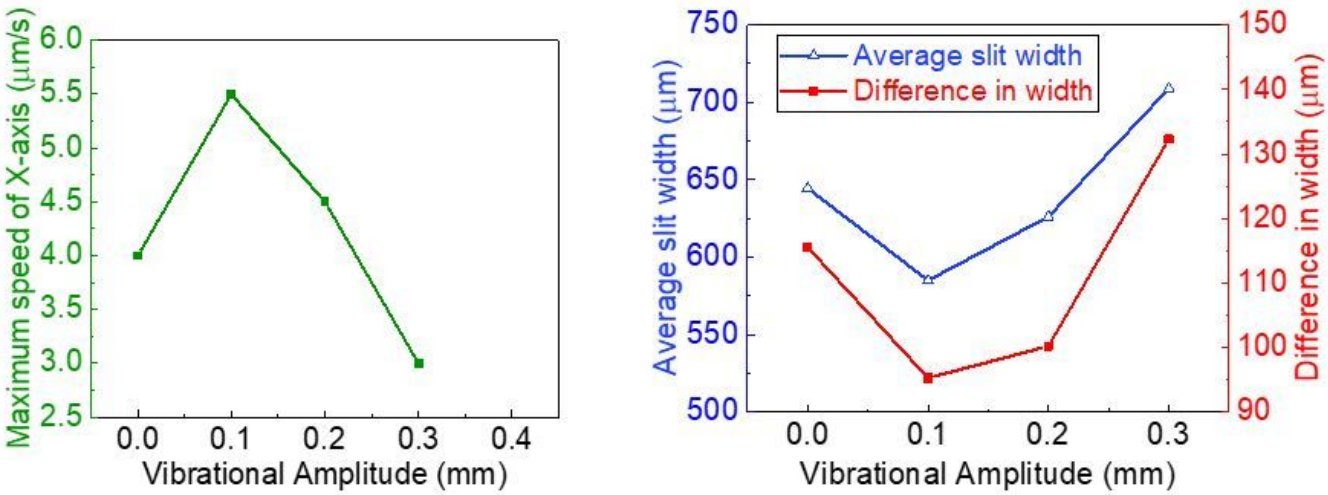

(a) Maximum speed of X-axis (b) Slit width

Figure 11

Variations in the maximum movement speed of X-axis and slit width with respect to vibrational amplitude.

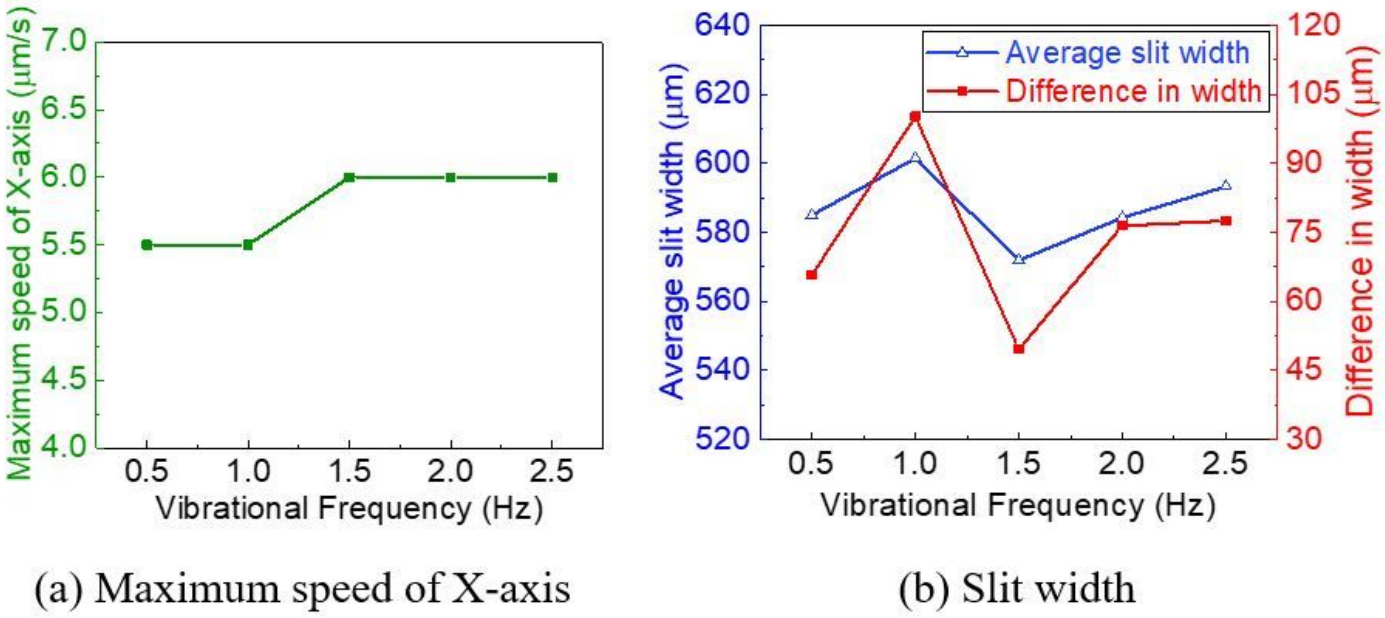

Figure 12

Variations in the maximum movement speed of X-axis and slit width with respect to vibrational frequency.

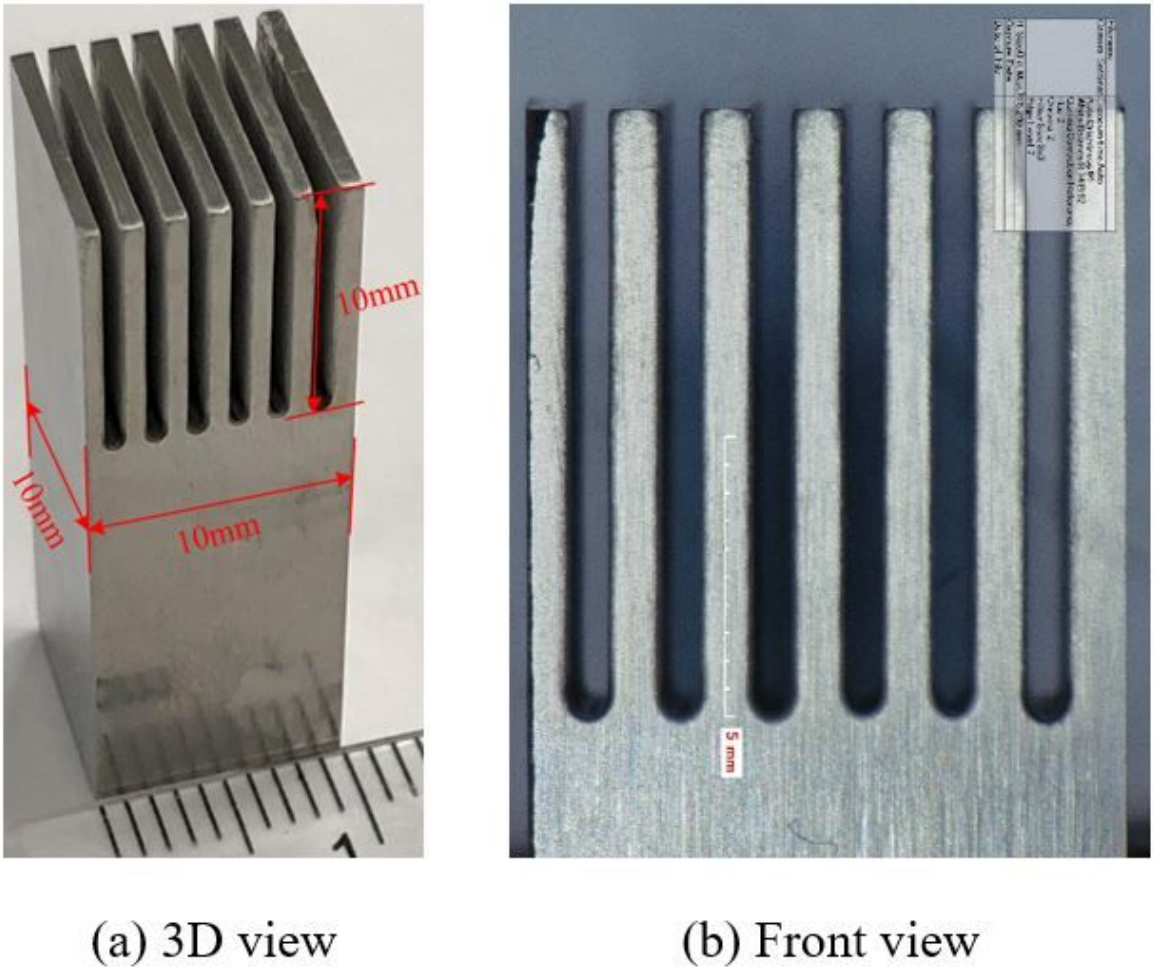

Figure 13

Array slice structure machined by workpiece vibration assisted electrochemical cutting: (a) 3D view, (b) front view.